Adsorption behaviour of Chrysoidine R dye on a metal/halide-free variant of ordered mesoporous carbon

Asna Mariyam[a], Jyoti Mittal[a], Farzeen Sakina[b], Richard T. Baker[b,*], Ashok K. Sharma[c]

[a]*Department of Chemistry, Maulana Azad National Institute of Technology, Bhopal 462 003, India,*
emails: asna.maryam1995@gmail.com (A. Mariyam), jyalmittal@yahoo.co.in (J. Mittal)
[b]*Department of Chemistry, University of St. Andrews, St. Andrews, Fife KY16 9AJ, United Kingdom,*
Tel. +441334463899; Fax: +441334463808; email: fs43@st-andrews.ac.uk, rtb5@st-andrews.ac.uk
[c]*Department of Chemistry, Deenbandhu Chhotu Ram University of Science and Technology, Murthal, Sonipat 131039,*
India, email: ashokksharma2k18@gmail.com

ABSTRACT

The paper reports the removal of Chrysoidine R, a toxic mono-azo dye from its aqueous solution by employing metal- and halide-free variant of ordered mesoporous carbon as adsorbent in batch experiments. The influence of various parameters such as hydronium ion concentration, adsorbent dosage, initial dye concentration, exposure time on dye uptake was studied. The process could be described by Langmuir, Freundlich and Dubinin-Radushkevitch isotherm models. Evaluation of thermodynamic variables proved that the adsorption was spontaneous, feasible and endothermic. The kinetics involved in the process was worked out using pseudo-first-order and pseudo-second-order kinetic models. The latter was found appropriate for the analysis of the experimental data. The mechanism governing the overall adsorption was elucidated with the aid of various mathematical models. The adsorption was found to proceed via film diffusion with chemisorption being the rate-determining step. The complete removal of dye with fast removal rate makes the material propitious in the field of water treatment.

Keywords: Chrysoidine R; Adsorption isotherms; Kinetics; Pseudo-second-order; Film diffusion; Ordered mesoporous carbon

1. Introduction

Contamination of natural water resources is a gross global problem which has always been a source of motivation for researchers to develop strategies that are not only effective, but also economical. For eons, various water treatment techniques are in practice [1–4]. There is a wide variety of water contaminants that destroy the aqueous environment and deteriorate water quality [5]. As far as the composition of textile effluents is concerned, its major part is constituted by synthetic organic dyes [6,7]. Among various physicochemical methods for the treatment of dye-polluted water, adsorption is considered as one of the most efficient techniques [8] due to ease of operation, low investment costs and no noxious repercussions [9]. Owing to the stability of aromatic ring present in their skeleton, the dyes are intractable and their treatment by various chemical and biological methods, their degradation is extremely difficult and may lead to the formation of even more toxic products. This is where treatment of dye-polluted waters by adsorption seems to be the saviour.

Azo dyes are highly water-soluble and form the largest group of dyes that are mainly employed for dyeing purposes in textile industries [10]. Most of these are carcinogenic and their precursors, aromatic amines (formed on cleavage) are also well-known carcinogens. An expansive

* Corresponding author.

range of adsorbents has been used in the field of waste-water remediation. They are broadly classified as low-cost adsorbents [11] and commercially available adsorbents [12], the former class includes poultry wastes [13,14], agricultural wastes [15] such as rice husk [16], coconut husk [17], undesirable weeds [18], de-oiled soya [19], etc., industrial wastes such as fly ash [20], bottom ash, [19], saw dust [21], etc. The other class comprises silica gel [22], zeolites [23], alumina gel [24] and activated carbon [25]. It has been more than a couple of decades since the interest of researchers has shifted from activated carbon to ordered mesoporous carbon as adsorbent due to their exceptional properties like high surface area and degree of meso-porosity, alterable pore sizes, faster reaction rates and excellent adsorption capacities [26].

The ordered mesoporous carbon was first synthesized by Ryoo et al. [27] by nano-casting. Since then, a large number of synthesis methods have been adopted for their preparation [28]. The present material, which is a metal- and halide-free variant of ordered mesoporous carbon, has been synthesized by base-catalysed two-phase separation, adopting the method proposed by Sakina and Baker [29]. Most of the times, when metal hydroxide and halogen acid are used to catalyse polymerization and condensation reactions, respectively, the traces of them remain in the final product. This would lower their efficiency if used as adsorbent and also as support in heterogeneous catalysis, by blocking the active sites in case of the former and by poisoning the final product in latter case. Herein, metal- and halide-free variant of ordered mesoporous carbon was synthesized by the use of ammonium hydroxide as a substitute of metal hydroxide and oxalic acid as a substitute of halogen acid for polymerization and condensation reactions, respectively.

The potential of the material as a dye adsorbent was investigated by choosing Chrysoidine R as adsorbate. Chrysoidine R (Fig. 1), also known as Basic Orange 1, is a synthetic mono-azo textile dye. Once reduced, it can undergo subsequent chain reactions to form toxic compounds. If administered orally, it has potential to cause carcinomas, liver-cell adenomas and leukaemia in animals. Moreover, some case studies have suggested its carcinogenicity as well [30]. Present paper is a first ever report to remove the dye Chrysoidine R using metal/halide-free ordered mesoporous carbon (OMC).

2. Experimental methods

2.1. Synthesis of ordered mesoporous carbon

The synthesis of metal/halogen free OMC material was done similar to the method reported by Sakina and Baker [29]. Concisely, formaldehyde and resorcinol were
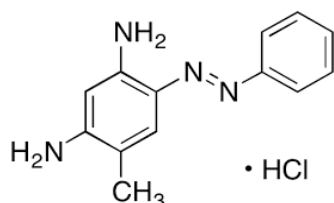
allowed to react prior to the addition of polymerization catalyst, ammonium hydroxide. The second step of condensation was marked by the addition of a structure-directing agent (F127) and oxalic acid as catalyst under uninterrupted stirring. The clear solution turned hazy that marked phase separation. After further stirring for about an hour, product was left for 12 h when polymer gel phase was formed. The product thus obtained was dried and cured at 80°C for a definite period of time, followed by its carbonisation at 400°C in an inert atmosphere.

2.2. Material characterization

The characterization of the prepared material was carried out by small angle X-ray diffraction (SAXRD), nitrogen physisorption experiments and transmission electron microscopy. Cu Kα radiation in a PANalytical Empyrean instrument was used to obtain SAXRD diffractograms. Micrometrics TriStar II 3020 instrument was used to record nitrogen sorption isotherms after degassing the samples at 120°C in vacuum for 12 h. The data on Barrett, Joyner, Halenda pore size distribution was obtained from physisorption experiments. Transmission electron microscopy (TEM) samples were prepared by ultrasound-aided suspension of ordered mesoporous carbon in acetone and tweezers were used to swipe the carbon-coated copper grid through it. The grids were dried using halogen lamp for about 12 h which were then examined using electron microscope JEOL 2011, provided with a filament of lanthanum hexaboride (200 kV). The images obtained were studied via Digital Micrograph software.

2.3. Adsorption studies

Analytical reagent grade Chrysoidine R chemically named as, 2,4-diamino-5-methylazobenzene (molecular formula and molecular weight are $C_{13}H_{15}ClN_4$ and 262.74 g/mol, respectively) was obtained from M/s Merck and used as received. All batch experiments were carried out using double distilled water. A digital pH meter with in-built microprocessor (M/s Henna Instruments, Italy) was used to measure the pH at various stages. The absorbance and thus the dye concentration in the solution, pre- and post-adsorptions were monitored using UV-Vis spectrophotometer by EI, India. All the observations were recorded at maximum absorption wavelength (λ_{max}) of 449 nm of Chrysoidine R.

All the studies were carried out in batch mode in isothermal surroundings at 30°C temperature. Definite volumes of dye solution (20 mL), differing in concentration (1×10^{-5} to 1×10^{-4} M) were poured into Erlenmeyer flasks with 100 mL capacity and the pH adjustments (2–11) were made using 0.1 M NaOH and 0.1 M HCl solutions. The solutions with pre-determined absorbance were shaken in sporadic manner with suitable quantity of adsorbent added to each flask. The flasks were allowed to shake until the attainment of equilibrium. The mixtures were then centrifuged and the absorbance of supernatant was recorded spectrophotometrically at 449 nm and pH 7.0. The equilibrium adsorption capacity was evaluated by the following formula:

$$q_e = \frac{(C_0 - C_e)V}{w} \tag{1}$$

Fig. 1. Structure of Chrysoidine R.

where C_0 and C_e refer to the pre-adsorption and the equilibrium concentration of dye (mol/L), respectively, V is the volume of solution mixture (L) and w is the weight (g) of the adsorbent used.

In order to carry out adsorption isotherm and adsorption kinetics studies, known amount of OMC was mixed with 20 mL volume of dye solution of optimized concentration value obtained during preliminary studies and shaken isothermally, at 30°C, 40°C and 50°C, respectively, on a water bath shaker. The solution mixtures (with definite adsorbent amount) were withdrawn at regular intervals to record the absorbance of the supernatant, obtained after decantation, using UV/Vis spectrophotometer. Thus, final concentration of each dye solution was evaluated and accordingly different isothermal and kinetic models were verified for all the samples.

3. Results and discussion

3.1. Adsorbent characterization

The ordered mesoporous carbon was fundamentally amorphous due to calcination at 400°C [31], but the mesopores were sufficiently ordered to give XRD diffractograms with peaks observed at low 2θ angles. The reflections corresponding to Miller planes 100, 200, 210 of meso-structure consisting of 2-D hexagonal parallelly arranged cylindrical mesopores were obtained. The value of unit cell dimension as estimated from the positions of small angle X-ray diffraction peaks was found as 13.0 nm. The nature of nitrogen physisorption isotherm was Type IV, with distinctly visible capillary condensation in the relative pressure range of 0.4–0.8. The textural properties like specific surface area and pore volume and pore diameter were evaluated to be 608 m²/g and 0.63 cm³/g, respectively. The physisorption data were also used to evaluate the pore size distribution and a sharp peak corresponding to narrow pore size distribution was obtained. Thus, the material was found to have a uniform pore size distribution with an average pore diameter of 7.0 nm. TEM images at different magnifications showed extensive ordering of mesopores. The carbon-rich array in the images appeared dark and the mesopores appeared bright.

3.2. Preliminary studies

3.2.1. Influence of pH

The influence of pH on the uptake of Chrysoidine R by OMC was evaluated in the range of 2–11. There was a rapid rise in percentage removal of the dye when the pH was increased from 2.0 (42%) to 6.0 (93.5%), which can be observed in Fig. 2. The amount of dye adsorbed reached its maximum when the pH of the medium was neutral (98%) and there was a marginal decrease in the removal percentage above 7.0. Thus, all the ensuing experiments were made in neutral medium.

The abrupt rise in percentage removal or the dye adsorbed with an initial increase in pH is due to competition for adsorption between hydronium ions and the cationic dye. The increase in pH results from a decrease in hydronium ions in the medium, thereby decreasing the magnitude of competitive adsorption and maximizing the cationic dye adsorption onto the surface. Moreover, the repulsion between the protonated dye and positively charged surface in low pH prevents the efficient removal of dye by the adsorbent as the pH_{pzc} of the ordered mesoporous carbon, as determined from the salt addition method [32] was found to be 6.0 (pH < pH_{pzc} — positively charged surface; pH > pH_{pzc} — negatively charged surface). The removal percentage was the highest at neutral pH and higher in alkaline conditions than in acidic environment. The similar trend was observed elsewhere also [33].

3.2.2. Influence of adsorbent dosage

The appropriate dose of adsorbent to employ, in order to achieve maximum adsorption, was obtained by studying the effect of its amount on dye adsorption over the range of 5–10 mg. Fixed volumes of dye solution of a known concentration were shaken in different flasks containing different amounts of ordered mesoporous carbon. The removal percentage improved when the dose was increased from 6 mg (98%) to 10 mg (99.7%) and remained unaffected beyond it.

The improvement in removal percentage is attributed to the increase in adsorption active sites with increase in the amount of ordered mesoporous carbon and also their easy accessibility. No noticeable change in removal percentage beyond 10 mg and its sufficiency reveals that the amount is enough to cater for the used concentration of dye.

3.2.3. Influence of initial dye concentration

The effect of dye concentration was studied at pH 7.0 in the range from 1×10^{-5} M to 1×10^{-4} M where 20 mL of different concentration solutions were periodically shaken with 10 mg of the adsorbents for a definite period of time. The initial dye concentration effect study as shown in Fig. 3, revealed that initially, when the concentration was increased from 1×10^{-5} M to 6×10^{-5} M, the Chrysoidine R uptake by the ordered mesoporous carbon also increased. Further rise in concentration, however,
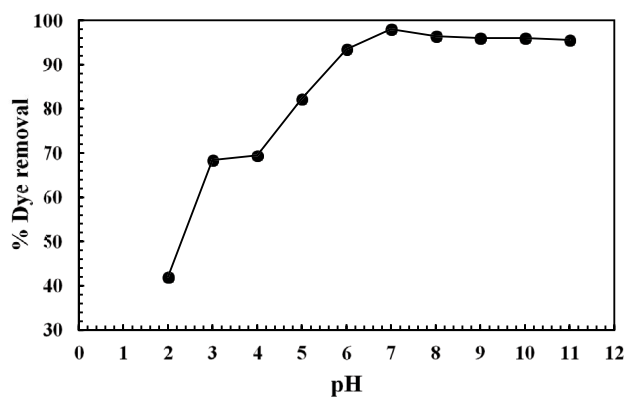
Fig. 2. Effect of pH on the adsorption of Chrysoidine R over OMC at 30°C (dye concentration = 6×10^{-5} M, adsorbent dose = 10 mg/20 mL).
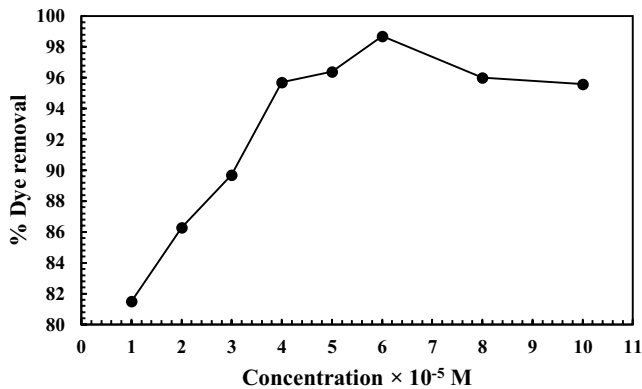
Fig. 3. Effect of concentration of Chrysoidine R on adsorption over OMC at 30°C (pH = 7, adsorbent dose = 10 mg/20 mL).

did not enhance the adsorption and in fact, a marginal decrease was observed after which the curve flattened.

At first, when the concentration was increased, the built-up concentration gradient across the adsorbate–adsorbent interface acts as a driving force for mass transfer from the solution phase to the adsorbent phase. It seems that at concentrations above 6×10^{-5} M, the adsorbate–adsorbate interactions at the interface, becomes pronounced to prevent efficient adsorption of the dye. Thus, the concentration of 6×10^{-5} M was chosen for carrying out the subsequent studies.

3.2.4. Influence of time of phase contact

The time required to attain equilibrium was evaluated by subjecting 20 mL dye solution and 10 mg adsorbent mixtures to periodic shaking and their withdrawal at 15 min intervals to analyze the amount adsorbed with time. The pH of the medium and the dye concentration were fixed as 7.0 and 6×10^{-5} M, respectively. The sharp rise in removal percentage during the first 15 min is due to smooth diffusion of dye molecules to the readily accessible, vacant surface sites of the adsorbent. Thereafter, the increase in removal percentage is gradual until the flattened curve, indicating the state of equilibrium is obtained. The gradual rise is owed to the limited available vacant sites due to their occupancy by the previously adsorbed molecules.

3.3. Adsorption isotherm studies

Isotherm studies form an integral part of adsorption system of any sort. In the present study, the applicability of four types of isotherm models, namely Langmuir, Freundlich, Temkin and Dubinin-Radushkevitch isotherms, was investigated [34–36]. Langmuir model is based upon certain assumptions that the adsorbent bears homogeneous surface and the adsorption proceeds by the formation of monolayer of the adsorbate ions and also, there is no mutual interactions of the adsorbate species. The linearized Langmuir isotherm equation is expressed as:

$$\frac{1}{q_e} = \frac{1}{q_0} + \frac{1}{bq_0 C_e} \tag{2}$$

where q_e refers to the equilibrium capacity of adsorption (mol/g), q_0 denotes the maximum adsorption capacity per unit mass of the ordered mesoporous carbon (mol/g), b represents the energy of adsorption (L/mol) and C_e is the molar concentration of dye at equilibrium (mol/L).

The linear plots of Eq. (2) with regression coefficient value almost equal to unity were obtained at all three temperatures viz. 30°C, 40°C and 50°C (Fig. 4). This indicates that Chrysoidine R forms monolayer on the surface of the ordered mesoporous carbon with no adsorbate species mutually interacting. The Langmuir constant values at different temperatures are presented in Table 1.

The experimental data were further analyzed using Freundlich isotherm which is based on the postulate that the interactions between the adsorbate ions adsorbed on the surface affect the binding affinities of the active sites. As a result, strong affinity sites are first to be occupied. Moreover, Freundlich isotherm favours adsorption non-ideal, multi-layer adsorption on heterogeneous surface. The isotherm was plotted based on the following expression:

$$\log q_e = \log K_F + \left(\frac{1}{n} \right) \log C_e \tag{3}$$

where K_F and n are the Freundlich constants (Table 1) representing the strength of adsorption and the intensity of adsorption, respectively, and the latter is also employed to study the favourability of reaction. A good fit of data to Freundlich adsorption isotherm suggests that the dye uptake involves both mono- and multi-layer adsorption (Fig. 5).

The possibility of indirect interactions between the adsorbate species was investigated by applying Temkin adsorption isotherm to the experimental data. The equation is represented as:

$$q_e = k_1 \ln k_2 + k_1 \ln C_e \tag{4}$$

where k_1 represents the heat of adsorption and k_2 corresponds to the binding constant at equilibrium (Table 1). Low regression coefficient values at all temperatures for q_e vs. $\ln C_e$ plot indicated that the on-going adsorption process cannot be described by it.

Fourth adsorption model, i.e., Dubinin-Radushkevitch model when applied to the data gave linear plots with good regression coefficient values at all temperatures (Fig. 6). The expression of D-R adsorption isotherm is:

$$\ln q_e = \ln q_m - \beta \in^2 \tag{5}$$

where q_m is the maximum amount of dye adsorbed (mol/g), β is the activity coefficient (Table 1), used to calculate the mean sorption energy, E ($=1/\sqrt{-2\beta}$) and $\in$ is the Polanyi potential and it is expressed as:

$$\in = RT \left(1 + \frac{1}{C_e} \right) \tag{6}$$

The significance of this isotherm model lies in the fact that the calculated value of mean sorption energy helps in distinguishing between physisorption and chemisorption
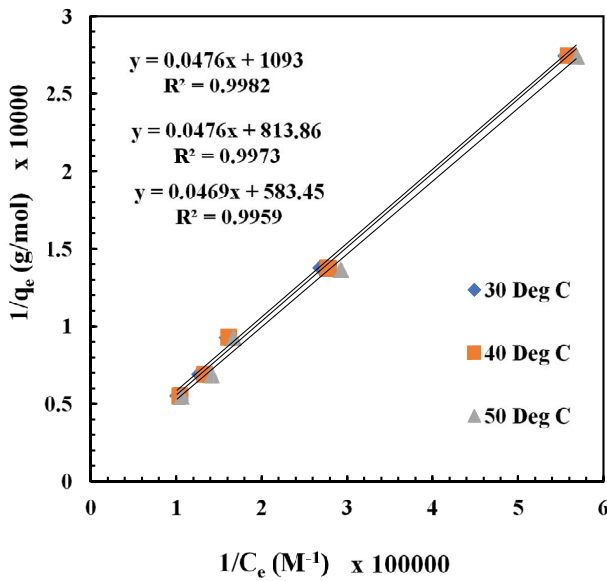
Fig. 4. Langmuir adsorption isotherm for Chrysoidine R–OMC system at different temperatures (pH-7.0; adsorbent dosage-10 mg/20 mL).
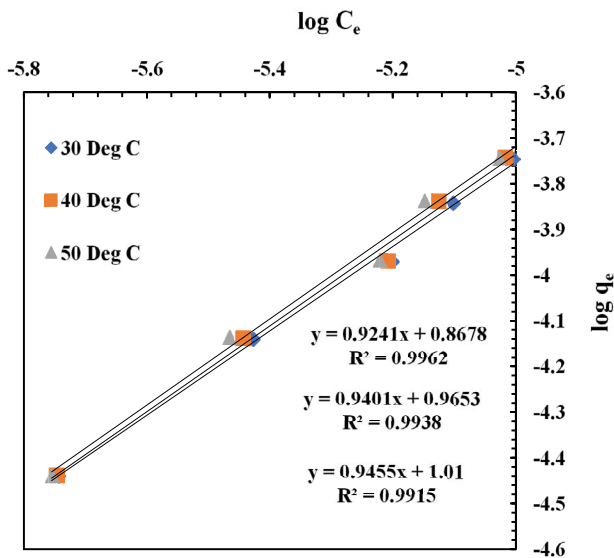
Fig. 5. Freundlich adsorption isotherm for Chrysoidine R–OMC system at different temperatures (pH-7.0; adsorbent dosage-10 mg/20 mL).

processes [37]. The values lower than 8 kJ/mol and in the range of 8–16 kJ/mol are indicative of physisorption and chemisorption, respectively. The values greater than 8 kJ were obtained at all temperatures (9.12 kJ/mol at 30°C, 9.12 kJ/mol at 40°C, and 10.00 kJ/mol at 50°C), indicating thereby the involvement of chemisorption in the present case.

3.4. Calculation of thermodynamic parameters

The evaluation of thermodynamic parameters like Gibb's free energy ($\Delta G°$), enthalpy ($\Delta H°$), entropy ($\Delta S°$)
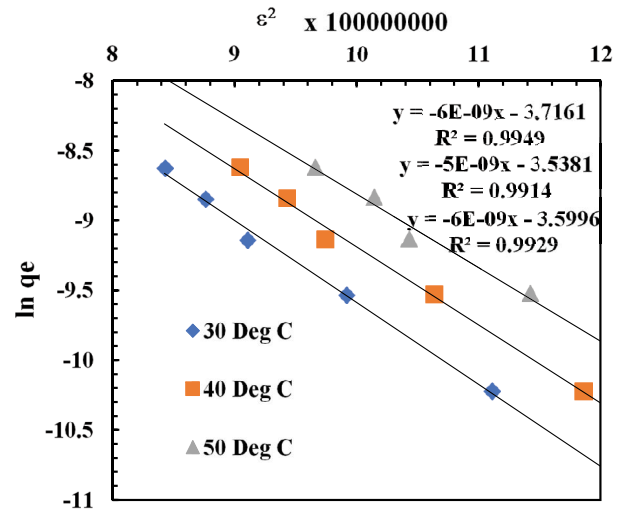
Fig. 6. Dubinin–Radushkevitch adsorption isotherm for Chrysoidine R–OMC system at different temperatures (pH-7.0; adsorbent dosage-10 mg/20 mL).

helps to study the spontaneity, nature and mutual affinities of adsorbent–adsorbate, respectively. The Langmuir constant 'b' was used to calculate the abovementioned thermodynamic parameters by employing the following well-founded relations:

$$\Delta G° = -RT \ln b \tag{7}$$

$$\Delta H° = -R\left(\frac{T_2 T_1}{(T_2 - T_1)}\right) \times \ln\left(\frac{b_2}{b_1}\right) \tag{8}$$

$$\Delta S° = \frac{(\Delta H° - \Delta G°)}{T} \tag{9}$$

where R (J/mol K) and T (K) have their conventional meanings.

The negative values of Gibb's free energy at all three temperatures predict the spontaneity and feasibility of the on-going reaction. The positive values of enthalpy indicate that the adsorption of Chrysoidine R on OMC is an endothermic reaction which is also verified by the increment in equilibrium adsorption capacity with temperature (Tables 1 and 2). The calculated entropy is also a positive value, indicative of progress of adsorption with an increase in randomness at the solid–solution interface.

The separation factor 'r' given by Chakraborty and Weber [38] also gives an idea about the favourability of the reaction.

$$r = \frac{1}{1 + bC_0} \tag{10}$$

where C_0 is the initial concentration of dye (mol/L). For $r > 1$, $r = 1$, and $r = 0$, the process is considered as unfavourable, linear and irreversible, respectively, and a value in the range $0 \leq r \leq 1$ refers to a favourable reaction. Herein,

the values of 'r' (lower than unity) at all temperatures correspond to the process favourability (Table 2).

3.5. Kinetics of adsorption

Studying the kinetics of adsorption helps in determining the effect of experimental variables on adsorption rate and the determination of rate-controlling step is also based on the data obtained in kinetic studies. For the analysis of kinetic data and the determination of specific rate constants, pseudo-first-order equation, also known as Lagergren's first-order equation (Eq. (11)) [39] and pseudo-second-order equation (Eq. (12)) [40] were employed.

$$\log\left(q_e - q_t\right) = \log q_e - \frac{k_1}{2.303} \times t \tag{11}$$

$$\frac{t}{q_t} = \frac{1}{k_2 q_e^2} + \frac{t}{q_e} \tag{12}$$

where q_e is the equilibrium adsorption capacity (mol/g); q_t is the adsorption capacity at any time 't' (mol/g); k_1

is the pseudo-first-order rate constant (min⁻¹); k_2 is the pseudo-second-order rate constant (g/mol min).

The pseudo-second-order plot of t/q_t vs. t, gave the best fit to the kinetic data with regression coefficient value almost equal to unity (>0.99) at all temperatures (30°C, 40°C and 50°C; Fig. 7). The slope and intercept values were used to evaluate the rate constant values which are listed in Table 1. The value of rate constant increased with temperature. The rate of adsorption also increased and the removal was 100% after just an hour at 50°C. The applicability of pseudo-second-order model suggests the involvement of chemisorption in the present case. The pseudo-second-order kinetic rate constant increased with temperature and the values were calculated to be 0.839×10^3, 2.853×10^3 and 5.998×10^3 g/mol min at 30°C, 40°C and 50°C, respectively. The faster adsorption rates at higher temperatures resulted in shortened half-life (19.84 min at 30°C; 5.84 min at 40°C; 2.51 min at 50°C).

3.6. Establishment of mechanism

The mechanism and the rate-controlling step were investigated by evaluating the kinetic data. The well-founded mathematical models by Boyd et al. [41] and Reichenberg [42] and the assumptions of Crank [43] were used to establish the mechanism involved in the adsorption of Chrysoidine R by the ordered mesoporous carbon. Following expressions were used to find out whether the uptake of dye proceeds via particle diffusion or film diffusion.

$$F = \frac{Q_t}{Q_\infty} \tag{13}$$

$$F = 1 - \frac{6}{\pi^2} \sum_\infty^1 \left(\frac{1}{n^2}\right) e^{\left(-n^2 B_t\right)} \tag{14}$$

$$B_t = \frac{\pi^2 D_i}{\left(r_0^2\right)} = \text{Time constant} \tag{15}$$

$$D_i = D_0 e^{\left(-\frac{E_a}{RT}\right)} \tag{16}$$

$$D_0 = \left(\frac{2.72 d^2 kT}{h}\right) e^{\frac{\Delta S^\#}{R}} \tag{17}$$

where Q_t and Q_∞ refer to the amount of dye adsorbed at time t and at equilibrium considering time taken to reach equilibrium as infinity; F, n, B_t, B, D_i refer to the fractional

Table 1
Values of various adsorption isotherm constants for the uptake of Chrysoidine R by OMC at different temperatures

Langmuir constants					
$q_0 \times 10^{-3}$ (mmol/g)			$b \times 10^4$ (L/mol)		
30°C	40°C	50°C	30°C	40°C	50°C
0.915	1.23	1.71	2.32	1.73	1.27
Freundlich constants					
n			K_F		
30°C	40°C	50°C	30°C	40°C	50°C
1.082	1.063	1.058	7.36	9.22	10.23
Temkin constants					
$k_1 \times 10^{-5}$			$k_2 \times 10^5$		
30°C	40°C	50°C	30°C	40°C	50°C
8.0	8.0	8.0	2.68	2.68	2.68
D-R constants					
q_m (mol/g)			$\beta \times 10^{-9}$		
30°C	40°C	50°C	30°C	40°C	50°C
0.024	0.027	0.029	6.00	6.00	5.00

Table 2
Values of various thermodynamic parameters for the adsorption of Chrysoidine R by OMC at different temperatures

Temperature (°C)	$-\Delta G°$ (kJ/mol)	$\Delta H°$ (kJ/mol)	$\Delta S°$ (JK/mol)	r Values
30	25.328	23.257	160.35	0.417
40	25.396	26.168	164.74	0.490
50	25.371	24. 666	154.91	0.567
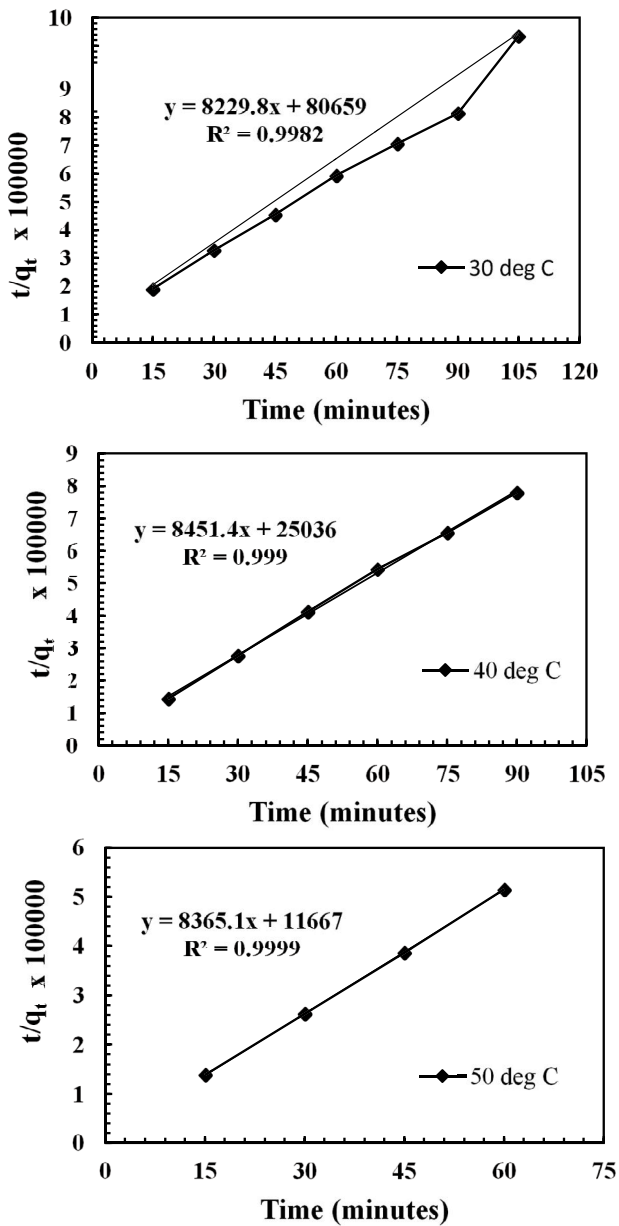
Fig. 7. Plot of time vs. t/q_t for Chrysoidine R–OMC system at different temperatures (pH-7.0; dye concentration-6 × 10⁻⁵ M; adsorbent dosage-10 mg/20 mL).

Fig. 8. Plot of B_t vs. time for Chrysoidine R–OMC system at different temperatures (pH-7.0; dye concentration-6 × 10⁻⁵ M; adsorbent dosage-10 mg/20 mL).

equilibrium attainment, Freundlich's constant, time constant, the value of which is obtained from Reichenberg's table, time constant whose value is obtained from the slope of B_t vs. time plot, and the diffusion coefficient, respectively. D_0, E_a, d, k, h, R, on the other hand, represent the maximum diffusion coefficient, activation energy (kJ/mol), distance between two nearest adsorbent surface sites, Boltzmann constant (1.38 × 10⁻²³ J/K), Plank's constant (6.62 × 10⁻³⁴ J s), universal gas constant, respectively.

The adsorption is assumed to proceed via three consecutive steps viz. (a) adsorbate ions diffuse to the adsorbent surface, which is called film diffusion, (b) diffusion of adsorbate ions/molecules within the porous structure of the adsorbent, referred to as particle diffusion, (c) adsorption of adsorbate on the internal adsorbent surface. The last step is assumed to proceed too fast to be rate controlling. Thus, only one of the first two steps, i.e., film diffusion and particle diffusion can be rate determining. The rate-determining step is worked out by the following possible cases: if the rate of external transport exceeds that of internal transport, the process is assumed to proceed predominantly by film diffusion (External Transport > Internal Transport), whereas, the involvement of particle diffusion is predicted when the case is opposite, i.e., Internal Transport > External Transport. In the third case where the rates of both internal and external transport are almost equal, the liquid film formation at the solution and solid surface junction does not allow further transport of adsorbate to the surface at a considerable rate.

The plot of B_t vs. time was used to determine the operating mechanism. In this study, the linear plots obtained did not pass through the origin suggesting that adsorption proceeds through film diffusion (Fig. 8). These results were validated by linear graph obtained for log(1 − F) vs. time plot (Fig. 9). The values of diffusion coefficients obtained from slope of B_t vs. time plot at 30°C, 40°C and 50°C have increased with temperature. It is basically due to reduction in frictional force at high temperatures resulting in improved mobility of ions. The diffusion coefficient values are recorded in Table 3. The slope value of $\ln D_i$ vs. $T^{-1}(K^{-1})$ plot was used for the calculation of activation energy (Fig. 10). High value of activation energy (14.398 kJ/mol) and positive value of entropy indicates that the adsorption involved chemisorption and the affinity of adsorbate towards the adsorbent, respectively.

4. Conclusion

A metal/halide-free variant of ordered mesoporous carbon was examined for its potential to adsorb a toxic,

Time (minutes)
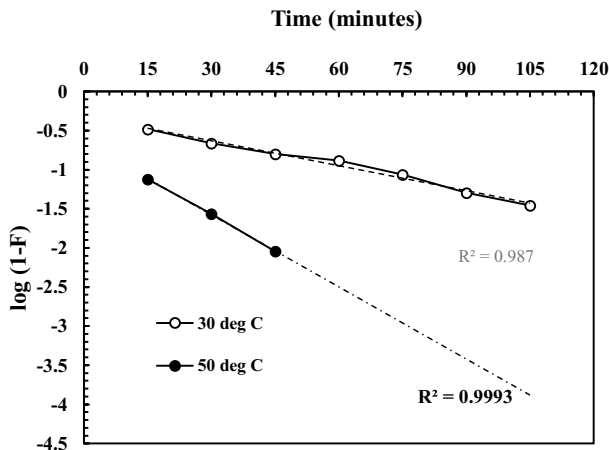
Fig. 9. Plot of log(1–*F*) vs. time for Chrysoidine R–OMC system at different temperatures (pH-7.0; dye concentration-6 × 10^{-5} M; adsorbent dosage-10 mg/20 mL).
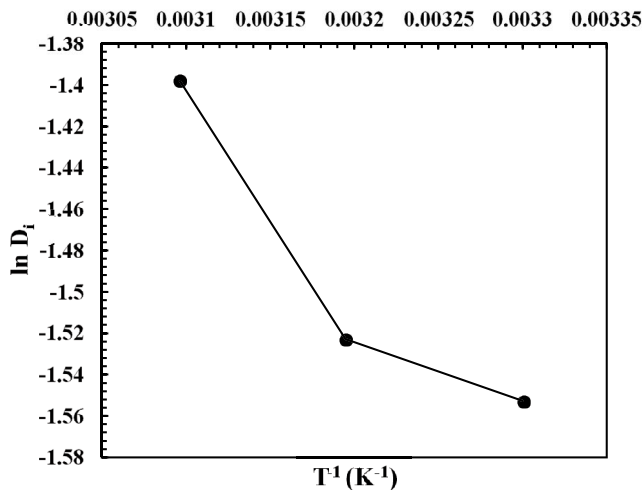
Fig. 10. Plot of lnDi vs. T^{-1} (K–1) for Chrysoidine R–OMC system at different temperatures (pH-7.0; dye concentration-6 × 10^{-5} M; adsorbent dosage-10 mg/20 mL).

Table 3
Values of diffusion coefficients (D_i and D_0), energy of activation (E_a) and entropy ($\Delta S^{\sharp}$)

D_i (m²/min)			D_0 (m²/min)	E_a (J/mol)	$\Delta S^{\sharp}$ (JK/mol)
30°C	40°C	50°C			
2.8 × 10^{-2}	3 × 10^{-2}	4 × 10^{-2}	8.23	14,398.65	42.15

mono-azo dye Chrysoidine R. The conditions of optimum adsorption were obtained. The Langmuir, Freundlich and Dubinin-Radushkevitch isotherm models suited well to the experimental data. The values of thermodynamic variables revealed the spontaneity and endothermicity of the process. Kinetics of the adsorption was studied. The fitting of kinetic data to pseudo-second-order model indicated that chemisorption was the rate-determining step. There was complete dye removal at 50°C in just an hour. It was

found from mass transfer studies that the adsorption proceeds via film diffusion. The results reported in the present work are good enough to conclude that the ordered mesoporous carbon is a promising dye adsorbent.

Acknowledgements

References

[1] A.E. Ghaly, R. Ananthashankar, M. Alhattab, V.V. Ramakrishnan, Production, characterization and treatment of textile effluents: a critical review, J. Chem. Eng. Process Technol., 5 (2014) 1–19.

[2] P. Rajasulochana, V. Preethy, Comparison on efficiency of various techniques in treatment of waste and sewage water–a comprehensive review, Resour.-Effic. Technol., 2 (2016) 175–184.

[3] D. Bhatia, N.R. Sharma, J. Singh, R.S. Kanwar, Biological methods for textile dye removal from wastewater: a review, Crit. Rev. Env. Sci. Technol., 47 (2017) 1836–1876.

[4] K. Vikrant, B.S. Giri, N. Raza, K. Roy, K.H. Kim, B.N. Rai, R.S. Singh, Recent advancements in bioremediation of dye: current status and challenges, Bioresour. Technol., 253 (2018) 355–367.

[5] T. Deblonde, C. Cossu-Leguille, P. Hartemann, Emerging pollutants in wastewater: a review of the literature, Int. J. Hyg. Environ. Health, 214 (2011) 442–448.

[6] D.A. Yaseen, M. Scholz, Textile dye wastewater characteristics and constituents of synthetic effluents: a critical review, Int. J. Environ. Sci. Technol., 16 (2019) 1193–1226.

[7] C. Fernández, M.S. Larrechi, M.P. Callao, TrAC, An analytical overview of processes for removing organic dyes from wastewater effluents, Trends Anal. Chem., 29 (2010) 1202–1211.

[8] S.D. Faust, O.M. Aly, Adsorption Processes for Water Treatment, Elsevier, 2016.

[9] I. Anastopoulos, A. Mittal, M. Usman, J. Mittal, G. Yu, A. Núñez-Delgado, M. Kornaros, A review on halloysite-based adsorbents to remove pollutants in water and wastewater, J. Mol. Liq., 269 (2018) 855–868.

[10] S. Sarkar, A. Banerjee, U. Halder, R. Biswas, R. Bandopadhyay, Degradation of synthetic azo dyes of textile industry: a sustainable approach using microbial enzymes, Water Conserv. Sci. Eng., 2 (2017) 121–131.

[11] A. Kausar, M. Iqbal, A. Javed, K. Aftab, H.N. Bhatti, S. Nouren, Dyes adsorption using clay and modified clay: a review, J. Mol. Liq., 256 (2018) 395–407.

[12] L. Luo, Y. Guo, T. Zhu, Y. Zheng, Adsorption species distribution and multicomponent adsorption mechanism of SO_2, NO, and CO_2 on commercial adsorbents, Energy Fuels, 31 (2017) 11026–11033.

[13] A. Mittal, M. Teotia, R.K. Soni, J. Mittal, Applications of egg shell and egg shell membrane as adsorbents: a review, J. Mol. Liq., 223 (2016) 376–387.

[14] J. Mittal, V. Thakur, A. Mittal, Batch removal of hazardous azo dye Bismark Brown R using waste material hen feather, Ecol. Eng., 60 (2013) 249–253

[15] S. Banerjee, M.C. Chattopadhyaya, Adsorption characteristics for the removal of a toxic dye, tartrazine from aqueous solutions by a low-cost agricultural by-product, Arabian J. Chem., 10 (2017) S1629–S1638.

[16] T.G. Chuah, A. Jumasiah, I. Azni, S. Katayon, S.T. Choong, Rice husk as a potentially low-cost biosorbent for heavy metal and dye removal: an overview, Desalination, 175 (2005) 305–316.

[17] A. Mittal, R. Jain, J. Mittal, M. Shrivastava, Adsorptive removal of hazardous dye quinoline yellow from wastewater using

coconut-husk as potential adsorbent, Fresenius Environ. Bull., 19 (2010) 1–9.

[18] H. Lata, V.K. Garg, R.K. Gupta, Removal of a basic dye from aqueous solution by adsorption using *Parthenium hysterophorus*: an agricultural waste, Dyes Pigm., 74 (2007) 653–658.

[19] V.K. Gupta, A. Mittal, V. Gajbe, J. Mittal, Adsorption of basic fuchsin using waste materials-bottom ash and de-oiled soya as adsorbents, J. Colloid Interface Sci., 319 (20078) 30–39.

[20] D. Sun, X. Zhang, Y. Wu, X. Liu, Adsorption of anionic dyes from aqueous solution on fly ash, J. Hazard. Mater., 181 (2010) 335–342.

[21] S.D. Khattri, M.K. Singh, Removal of malachite green from dye wastewater using neem sawdust by adsorption, J. Hazard. Mater., 167 (2009) 1089–1094.

[22] H.J. Wang, J. Kang, H.J. Liu, J.H. Qu, Preparation of organically functionalized silica gel as adsorbent for copper ion adsorption, J. Environ. Sci., 21 (2009) 1473–1479.

[23] J. Shi, Z. Yang, H. Dai, X. Lu, L. Peng, X. Tan, R. Fahim, Preparation and application of modified zeolites as adsorbents in wastewater treatment, Water Sci. Technol., 2017 (2018) 621–635.

[24] L.M. Camacho, A. Torres, D. Saha, S. Deng, Adsorption equilibrium and kinetics of fluoride on sol–gel-derived activated alumina adsorbents, J. Colloid Interface Sci., 349 (2010) 307–313.

[25] G. Mezohegyi, F.P. van der Zee, J. Font, A. Fortuny, A. Fabregat, Towards advanced aqueous dye removal processes: a short review on the versatile role of activated carbon, J. Environ. Manage., 102 (2012) 148–164.

[26] Z. Wu, D. Zhao, Ordered mesoporous materials as adsorbents, Chem. Commun., 47 (2011) 3332–3338.

[27] R. Ryoo, S.H. Joo, S. Jun, Synthesis of highly ordered carbon molecular sieves via template-mediated structural transformation, J. Phys. Chem. B, 103 (1999) 7743–7746.

[28] Y.T. Ma, L. Liu, Z.Y. Yuan, Direct synthesis of ordered mesoporous carbons, Chem. Soc. Rev., 42 (2013) 3977–4003.

[29] F. Sakina, R.T. Baker, Metal-and halogen-free synthesis of ordered mesoporous carbon materials, Microporous Mesoporous Mater., 289 (2019) 109622.

[30] V.M. Nurchi, M. Crespo-Alonso, R. Biesuz, R. Alberti, M.I. Pilo, N. Spano, G. Sanna, Sorption of chrysoidine by row cork and cork entrapped in calcium alginate beads, Arabian J. Chem., 7 (2014) 133–138.

[31] A.H. Lu, B. Spliethoff, F. Schüth, Aqueous synthesis of ordered mesoporous carbon via self-assembly catalyzed by amino acid, Chem. Mater., 20 (2008) 5314–5319.

[32] A.M. Cardenas-Peña, J.G. Ibanez, R. Vasquez-Medrano, Determination of the point of zero charge for electrocoagulation precipitates from an iron anode, Int. J. Electrochem. Sci., 7 (2012) 6142–6153.

[33] A. Mittal, Adsorption kinetics of removal of a toxic dye, Malachite Green, from wastewater by using hen feathers, J. Hazard. Mater., 133 (2006) 196–202.

[34] P.M. Mathias, R. Kumar, J.D. Moyer, J.M. Schork, S.R. Srinivasan, S.R. Auvil, O. Talu, Correlation of multicomponent gas adsorption by the dual-site Langmuir model. Application to nitrogen/oxygen adsorption on 5A-zeolite, Ind. Eng. Chem. Res., 35 (1996) 2477–2483.

[35] R.I. Masel, Principles of Adsorption and Reaction on Solid Surfaces (Vol. 3), John Wiley and Sons, 1996.

[36] A.W. Adamson, A.P. Gast, Physical Chemistry of Surfaces (Vol. 150), Inter-science Publishers, New York 1967, p. 150.

[37] N.D. Hutson, R.T. Yang, Theoretical basis for the Dubinin-Radushkevitch (DR) adsorption isotherm equation, Adsorption, 3 (1997) 189–195.

[38] W.T. Chakraborty, R.K. Weber, Pore and solid diffusion model for fixed bed adsorbents. J. Am. Inst. Chem. Eng, 20 (1974) 228.

[39] F.G. Helfferich, J.S. Dranoff, Ion Exchange, McGraw-Hill, New York, 1962, p. 624.

[40] Y.S. Ho, G. McKay, Pseudo-second order model for sorption processes, Process Biochem., 34 (1999) 451–465.

[41] G.E. Boyd, A.W. Adamson, L.S. Myers Jr., The exchange adsorption of ions from aqueous solutions by organic zeolites. II. Kinetics1, J. Am. Chem. Soc., 69 (1947) 2836–2848.

[42] D. Reichenberg, Properties of ion-exchange resins in relation to their structure. III. Kinetics of exchange, J. Am. Chem. Soc., 75 (1953) 589–597.

[43] J. Crank, The Mathematics of Diffusion Oxford at the Clarendon Press, 1956.